Journal of Thermal Analysis and Calorimetry (2019) 135:2935–2941
https://doi.org/10.1007/s10973-018-7613-0

DSC TOPEM® study of high-energy mechanical milling-driven amorphization in β-As_4S_4-based arsenicals

Oleh Shpotyuk[1,2] · Andrzej Kozdras[3] · Peter Baláž[4] · Zdenka Bujňáková[4] · Yaroslav Shpotyuk[5,6]

Received: 24 February 2018 / Accepted: 29 July 2018 / Published online: 14 August 2018

Abstract

Temperature-modulated DSC TOPEM® method was applied to study amorphization in directly synthesized high-temperature polymorph of tetra-arsenic tetra-sulfide β-As_4S_4 affected to high-energy mechanical milling in a dry mode with 100–600 min^{-1} rotational speeds. The appeared amorphous phase is shown to possess dual nature, being related to As-rich glassy-like substances with low- and high-temperature glass transition midpoints. In respect of DSC TOPEM® studies, the crystalline–amorphous heterogeneity of chemical environment around β-As_4S_4 crystallites results in incongruent double-peak melting revealed through two endothermic effects at ~ 305 °C and ~ 315 °C. Amorphous phase continuously generated under ball milling with increased rotational speed is identified as compositionally authentic to arsenic monosulfide, but different in medium-range order from stoichiometric As_2S_3. The overall amorphization in commercial arsenic sulfide prepared by direct synthesis from elemental constituents under high-energy ball milling occurs from two sources, these being high-to-low-T_g amorphous phase transformation and direct vitrification of β-As_4S_4 phase. These data testifies in favor of "shell" model treated solid-state amorphization in terms of defect generation in parent β-As_4S_4 phase, the amorphous substance being nucleated heterogeneously from grain boundaries followed by stretching into crystalline grain interior.

Keywords Solid-state amorphization · Mechanical milling · Arsenic sulfide · DSC

Introduction

Generation a large variety of structural defects under high-energy ball mechanical milling (MM) [1–5] is known as an alternative technological resolution allowing approaching high-entropy amorphous state of parent crystalline substances, even those possessing extremely low glass-forming ability [6]. To a great extent, this unique phenomenon concerns a large group of overstoichiometric arsenic sulfides As-S with promising anticancer functionality guided due to MM-induced nanostructurization, also termed in biomedicine as arsenicals (nanoarsenicals) [7–11]. Different types of crystallization–vitrification processes in arsenical-based crystalline–amorphous systems were successfully studied employing the DSC method [12–15]. Recently [16], some of current authors reported first results on complete amorphization in partially crystalline $As_{45}S_{55}$ alloy prepared by direct synthesis from pure elements, this research being performed employing multifrequency DSC TOPEM® method. Amorphous substance appeared due to

✉ Oleh Shpotyuk
olehshpotyuk@yahoo.com

1 Jan Dlugosz University in Czestochowa, 13/15, al. Armii Krajowej, 42201 Czestochowa, Poland

2 Vlokh Institute of Physical Optics, 23, Dragomanov Str., Lviv 79005, Ukraine

3 Opole University of Technology, 75, Ozimska Str., 45370 Opole, Poland

4 Institute of Geotechnics of the Slovak Academy of Sciences, 45, Watsonova Str., 04001 Košice, Slovakia

5 Ivan Franko National University of Lviv, 107, Tarnavskogo Str., Lviv 79017, Ukraine

6 Centre for Innovation and Transfer of Natural Sciences and Engineering Knowledge, University of Rzeszow, 1, Pigonia Str., 35-959 Rzeszow, Poland

high-energy MM was shown to possess double-T_g relaxation originated from intrinsic separation on distinct high-temperature ($T_{g1} \cong 200$ °C) and low-temperature ($T_{g2} \cong 155.5$ °C) glassy-like components. This amorphous phase was identified with DSC TOPEM® as close to nominal alloy composition $As_{45}S_{55}$. Structural inspection with X-ray powder diffraction (XRPD) related to the first sharp diffraction peak (FSDP) revealed this phase as extension of melt-quenched As-rich glassy states stretching far beyond As_2S_3 stoichiometry.

Amorphous phase appeared in addition to crystalline counterpart has been detected when dealing with high-temperature polymorph of tetra-arsenic tetra-sulfide β-As_4S_4 prepared by direct synthesis from elemental constituents under high-energy wet or dry MM [17–19]. But chemical and thermodynamic authenticity of this phase has not been clarified up to now, and many controversies left in respect of its microstructure origin. In this work, we shall parameterize the amorphization effect in β-As_4S_4 arsenical, driven by high-energy MM under different rotational speeds, exploring heat capacity measurements with temperature-modulated DSC TOPEM®.

Experimental

Commercial arsenic sulfide β-As_4S_4 prepared by direct synthesis from elemental constituents (98% in purity, purchased in Sigma-Aldrich, USA) was used as a precursor for high-energy MM. Small pieces of this arsenical were coarse-grained powdered and sieved under 200 μm. Then, this powder (3 g) was subjected to MM in a dry mode under a protective Ar atmosphere, using planetary rotational ball mill Pulverisette 6 (Fritsch, Germany) loaded with 50 tungsten carbide balls of 10 mm in diameter. (The milling conditions were described elsewhere [18].) The overall MM duration was 60 min for each sample at different rotational speed n of the planet carrier, e.g., REHE-0 (non-milled or coarse-grained powdered sample sieved through 200 μm taken as a reference), REHE-100 ($n = 100$ min^{-1}), REHE-200 ($n = 200$ min^{-1}), REHE-500 ($n = 500$ min^{-1}) and REHE-600 ($n = 600$ min^{-1}). There was no possibility to measure directly the averaged temperature inside milling vial. Nevertheless, in respect of our estimates for other similar compounds, the highest temperature at $n = 600$ min^{-1} did not exceed 50 °C. In final, all samples were compressed by compacting inside a stainless steel die under the same pressure of ~ 0.7 GPa to prepare disk pellets (having 6 mm in a diameter and 1 mm in a thickness).

The calorimetric heat capacity measurements were taken with multifrequency DSC TOPEM® using DSC-1 calorimeter (Mettler-Toledo, Switzerland). In this method, the stochastic temperature modulations are superimposed on underlying rate of conventional DSC scans, resulting in distinguished frequency-dependent and frequency-independent phenomena [20, 21]. This provides more information concerning thermodynamic stability of the revealed phases, which is expected to be important in the case of phase-changed nanoarsenicals affected by high-energy MM. The DSC TOPEM® instrument was equipped with FRS5 + sensor and HT100 (Huber, Germany) intracooler, the STAR^e ver. 13a software being used to control experimental conditions and process the data. The calorimeter was multi-point calibrated using n-octane, Hg, In and Zn standard samples. The tested samples (ca. 9.5–12.0) were encapsulated in sealed 40-μL aluminum pans kept in protective N_2 atmosphere and scanned at the rate of 1.0 K min^{-1} stochastically modulated in pulses between 20 s and 60 s, the pulse height being 0.75 K. All TOPEM evaluations were adjusted using sapphire reference curve, the width and shift of calculation window being 60 s and 1 s, respectively. The heat capacity C_p measurements were taken in the range of 70–360 °C, each experiment protocol being averaged in triplicate.

Preliminary XRPD results [18] testified that MM-driven nanostructurization in β-As_4S_4 arsenical was revealed through extensive generation and interaction of nanoparticles (NPs) with character crystallite sizes of $d \sim 30$ nm for non-milled REHE-0 and REHE-100 samples, $d \sim 19$–21 nm for REHE-200–500 samples, and increased to $d \sim 25$–26 nm for REHE-600 sample. At the same time, within this sequence of samples, the average maximum strain demonstrated only growing tendency from 0.0043–0.0044‰ (REHE-0 and REHE-100) to 0.0082‰ (REHE-600) [18]. Thus, the arsenicals were not affected by MM under low rotational speed ($n = 100$ min^{-1}), while fragmentation of β-As_4S_4 crystallites (due to NPs aggregation) was prevailed under $n = 200$–500 min^{-1} speed. Finally, at $n = 600$ min^{-1}, the most energetically treated β-As_4S_4 crystallites agglomerated together, resulting in partially decreased (but not completely restored) specific surface area. It worth mentioning that evident growing tendency was observed with rotational speed n in amorphous halos in the experimental XRPD profiles of milled arsenicals starting from REHE-200 sample.

Results and discussion

Interphase transformations in binary As-S system have been in sphere of hot disputes for a long time, starting from first experimental observation addressed to Jonker more than a century ago [22]. In the earliest 1970s, the comprehensive calorimetric studies on overstoichiometric As-S alloys were performed by Hruby [23], who discovered the

second glass-forming region in this system ranging from 51 to 66 at.% of As. These experiments testified that crystalline As_4S_4 alloy as prepared by direct synthesis from elements is not chemically well-defined compound, but rather mixture of some phases. The melting process was shown to be incongruent [23], but it became congruent after annealing at 250 °C for 48 h, when this alloy was transformed in stable red-colored As_4S_4 crystalline modification with considerable amount of additional amorphous phase. This phase was ascribed to melt-quenched (MQ) glassy As_2S_3, as was suggested by Hruby [23], but without strict evidences (noteworthy, appearance of stoichiometric As_2S_3 is not allowed by simple chemical transformations in this alloy occurring only between overstoichiometric As_4S_4 compounds).

The variation of specific heat capacity C_{p0} in the reference (non-milled) coarse-grained powdered REHE-0 and MM REHE-500 pellets in high-temperature 295–320 °C and low-temperature 100–240 °C regions is depicted in Figs. 1 and 2, respectively. In the first heating run, two endothermic thermally induced melting effects are revealed in both samples, near ~ 305 °C and ~ 315 °C, testifying in a favor of incongruent melting (like it was suggested by Hruby [23]). The first of these effects is well detectable in C_{p0} due to strong peak T_{m1} at 304.1 °C observed in reference REHE-0 (black-solid curve, Fig. 1a), and more reduced peak at 303.2 °C detected in MM REHE-500 sample (red-dashed curve, Fig. 1a), i.e., at the liquidus of this alloy near arsenic monosulfide line [23]. The shape analysis testifies this peak is rather asymmetric in the reference sample, being completed from low-temperature side by evident shoulder near ~ 303.1–303.3 °C. Whichever the case, this endothermic effect occurs at peak temperature T_{m1}, which is less than T_m = 318 °C defined as

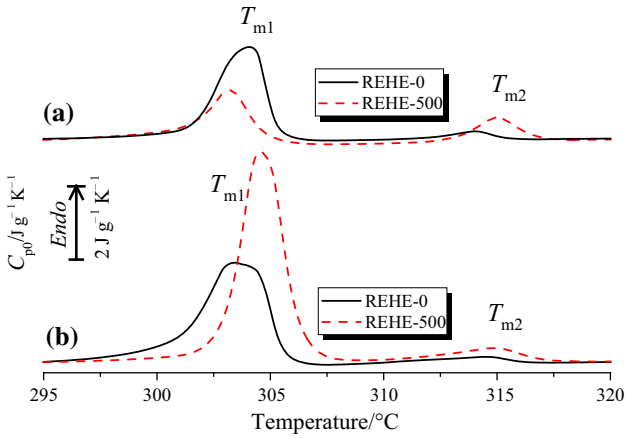

Fig. 1 Modulated DSC profile (TOPEM®) showing high-temperature variation of specific heat C_{p0} for coarse-grained powdered REHE-0 (black-solid curve) and MM REHE-500 (red-dashed curve) samples in the first (**a**) and second (**b**) heating runs

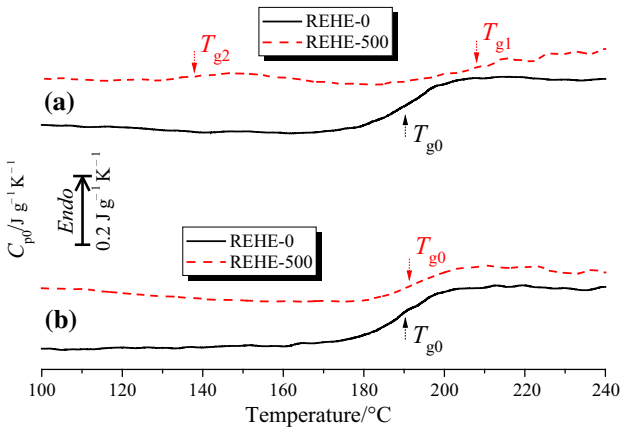

Fig. 2 Modulated DSC profile (TOPEM®) showing low-temperature variation of specific heat C_{p0} for coarse-grained powdered REHE-0 (black-solid curve) and MM REHE-500 (red-dashed curve) samples in the first (**a**) and second (**b**) heating runs

melting point for As_4S_4 by Blachnik [24], but very close to T_m = 307 °C defined by Street et al. [25] and T_m = 309 °C defined by Chattopadhya et al. [26] for this compound.

The second endothermic effect is less pronounced, but still quite detectable due to C_{p0} peak at T_{m2} in the same reference and MM β-As_4S_4 samples revealed themselves, respectively, at 314.0–315.0 °C. Noteworthy, the MM REHE-500 pellet possesses an obviously decreased first melting peak at T_{m1}, but increased second melting peak at T_{m2} as compared with the same in the reference sample (Fig. 1a). Hence, considerable redistribution in the intensities of these peaks accompanied by smaller changes in peaks positions (~ 1 °C decrease in T_{m1} and increase in T_{m2}) is the main result of high-energy MM effect on β-As_4S_4 arsenical.

The similar double-peak behavior was recently observed in melting of other overstoichiometric alloy in this As-S system, $As_{45}S_{55}$ composed of crystalline β-As_4S_4 and some amount of compositionally unknown amorphous phase with glass transition temperature T_g close to 165 °C [16]. The corresponding melting peak temperatures in this alloy were measured to be T_{m1} = 303.8 °C and T_{m2} = 317.4 °C, these effects being essentially non-elemental showing additional features from low-temperature side. Thus, the first C_{p0} peak (at T_{m1}) was completed with slight shoulder near 303.9 °C overlapped with broader hump in 302.7–305.5 °C domain, while second peak (at T_{m2}) revealed additional slight satellite pre-peak at 316.2 °C. The heating–cooling run allowed elimination second melting event (which therefore could be classified as irreversible), and all additional attributes from first one remaining only sharp single endothermic peak shifted to T_{m1} = 303.5 °C. (Similar changes were produced by MM resulting in complete amorphization of $As_{45}S_{55}$ alloy [16].) The double-peak C_{p0} effects were assumed to originate

from non-equilibrium melting of some crystalline compounds in principally different environments like crystalline and amorphous [27, 28]. Respectively, the melting of β-As_4S_4 in amorphous environment was accepted as responsible for endothermic peak at T_{m2} in $As_{45}S_{55}$ alloy [16]. This process was supplemented by strong effect at T_{m1} owing to melting of this well-separated phase near liquidus (mainly in its own environment). These interphase equilibria were essentially disturbed under high-energy MM, when β-As_4S_4 phase disappeared at a cost of amorphous substance, representing a mixture of two glassy phases possessing double-T_g relaxation at low- (T_{g1} = 155.5 °C) and high-temperature (T_{g2} = 197.9 °C) glass transition midpoints [16].

The modulated DSC profiles (TOPEM®) in Figs. 3 and 4 demonstrate respective first-run high-temperature variation of specific heat C_{p0} and non-reversing heat flow HF_{nrev} for MM REHE-200 (with fine aggregated crystalline NPs, d = ~19–21 nm [18]) and REHE-600 samples (with more agglomerated NPs, d = ~26 nm [18]) as compared with non-milled coarse-grained powdered REHE–0 probe (d ~ 30 nm [18]). The high-energy MM is always revealed in the melting temperature T_{m1} decrease, the effect, which is in strong dependence on average crystallite sizes d. Such melting-point depression is known to be most evident for nanostructurized substances with increased surface-to-volume ratio occurring under critical NPs sizes d (usually $d < 50$ nm) [29–31]. Assuming inverse quadratic nature of NPs size dependence in the melting equation, as it was accepted for covalently bonded semiconductor NPs by Farrell and Van Siclen [30]:

$$T_m = T_m^{\infty} \times \left(1 - (d_o/d)^2\right), \quad (1)$$

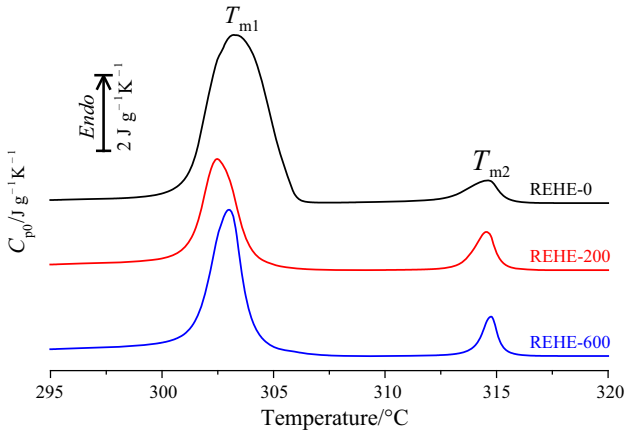

Fig. 3 Modulated DSC profile (TOPEM®) showing first-run high-temperature variation of specific heat C_{p0} for coarse-grained powdered REHE-0 (black curve), MM REHE-200 (red curve) and REHE-600 (blue curve) samples

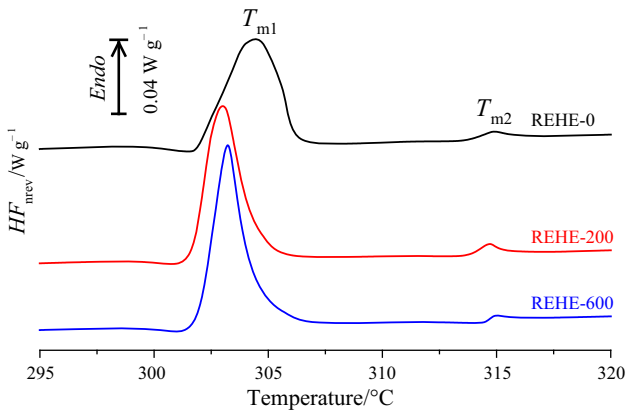

Fig. 4 Modulated DSC profile (TOPEM®) showing first-run high-temperature variation of non-reversing heat flow HF_{nrev} for coarse-grained powdered REHE-0 (black curve), MM REHE-200 (red curve) and REHE-600 (blue curve) samples

it can be calculated, accepting the data (Fig. 1) for REHE-0 (T_{m1} = 304.1 °C, d ~ 30 nm) and REHE-500 samples (T_{m1} = 303.2 °C, d ~ 20 nm), the melting temperature is close to 303.8 °C for MM sample with d ~ 25 nm crystallites, which is in excellent agreement with experimental melting peak position T_{m1} = 303.7 °C for REHE-600 sample (Figs. 3 and 4). With these data, the parameter T_m^{∞} in Eq. (1) which can be accepted as melting peak point for the bulk arsenical is estimated to be 304.8 °C, that is in very close proximity to T_{m1} = 304.5 °C, experimentally detected in the second heating run (i.e., after first melting) for REHE-500 pellet (Fig. 1b), when MM-driven nanostructurization is fully destroyed (due to re-melting). This melting-point depression effect in MM arsenicals parameterized in the extrapolated position T_{m1} and specific heat capacity ΔC_{p0} of the first melting peak in dependence on crystallite sizes d is illustrated by diagram in Fig. 5.

The appearance of additional amorphous phase was always detected in β-As_4S_4 prepared by direct synthesis

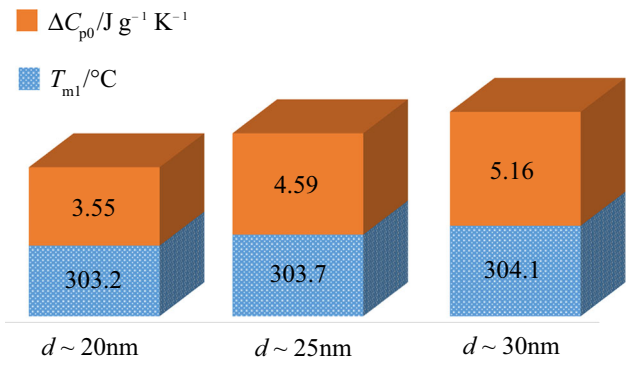

Fig. 5 Melting-point depression effect in directly synthesized β-As_4S_4 affected high-energy MM determined in the extrapolated position T_{m1} and specific heat capacity ΔC_{p0} of the first melting peak in dependence on crystallite sizes d

from elements [25], as well as in many other MQ and MM composites based on this arsenical [16–19, 32, 33]. This amorphization trend is clearly revealed in REHE-0 and MM REHE-500 pellets due to heat capacity C_{p0} variation in low-temperature 100–240 °C region (see Fig. 2). The first of these samples (coarse-grained powdered β-As_4S_4 arsenical) demonstrates strong relaxation effect with $\Delta C_{p0} = \sim 0.160$ J·g^{-1}·K^{-1} amplitude at glass transition midpoint $T_g = \sim 190.0$ °C. The second sample affected to high-energy MM shows double-T_g relaxation effect, the corresponding glass transitions obeying more fragile behavior at $T_{g1} = \sim 208.3$ °C ($\Delta C_{p0} = \sim 0.072$ J g^{-1} K^{-1}) and only slight specific heat C_p variation at $T_{g2} = \sim 130$–140 °C ($\Delta C_{p0} = \sim 0.020$ J g^{-1} K^{-1}).

Such double-T_g relaxation is known to be indicative of incomplete mixing or intrinsic phase separation in glassy systems [34, 35]. So it quite reasonable to assume appearance of two amorphous phases in MM β-As_4S_4 with high-temperature midpoint T_{g1} very close to that proper to MQ As_2S_3 [36, 37] and low-temperature midpoint T_{g2} near solidus of metastable melting in overstoichiometric As-S alloys determined by Hruby [23]. In general, an actual ratio between these amorphous phases reflects disturbance in a system due to created structural defects, so that different nature of the amorphized products follows from thermodynamic driven forces emerged under MM. That is why it seems only high-temperature amorphous phase with T_{g1} is reliably detectable in many experiments (as it occurred, e.g., in thermally annealed As_4S_4 alloy [23]), while full balance in the amorphized system is maintained by glassy phase with lower glass transition midpoint T_{g2}. Since the maximum T_g in binary As-S glassy system is achieved for stoichiometric As_2S_3 glass [36, 37], this additional amorphous phase is evidently also As-rich one (like it was in case of completely amorphized MM $As_{45}S_{55}$ alloy [16]).

With increased agglomeration of β-As_4S_4 crystallites, as it occurs at higher rotational speed n in REHE-600 sample (Fig. 6), the low-temperature relaxing glassy phase cannot be further simply determined, being masked by substantial growing trend in the low-temperature variation of specific heat C_{p0} just before glass transition ($T_{g1} = \sim 200.7$ °C, $\Delta C_{p0} = \sim 0.144$ J g^{-1} K^{-1}). This growing trend in the slope of specific heat C_{p0} curve is well observed as compared with DSC profiles for other samples shown in Fig. 5, such as REHE-0 ($T_{g1} = \sim 189.2$ °C, $\Delta C_{p0} = \sim 0.144$ J g^{-1} K^{-1}) and REHE-200 ($T_{g1} = \sim 189.8$ °C, $\Delta C_{p0} = \sim 0.113$ J g^{-1} K^{-1}). Correspondingly, the inner stress accumulated under high-energy MM relaxes more efficiently at higher rotational speeds n due to agglomeration of crystallites, as it can be well revealed from obviously decreasing low-temperature pre-T_g exotherm in non-reversing heat flow HF_{nrev} in Fig. 7 detected for REHE-600 pellet having larger β-As_4S_4 crystallites (d values approaching ~ 25 nm [18]).

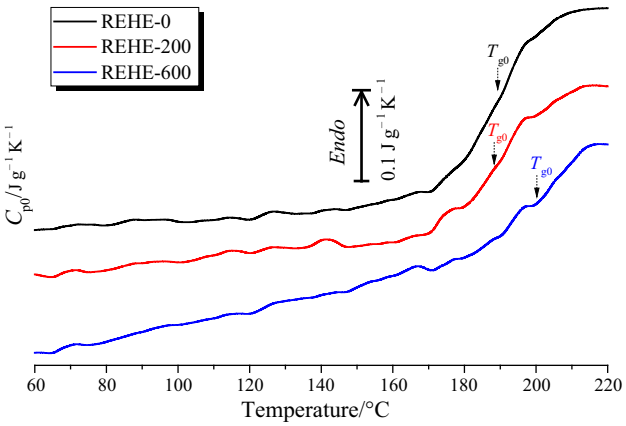

Fig. 6 Modulated DSC profile (TOPEM®) showing first-run low-temperature variation of specific heat C_{p0} for coarse-grained powdered REHE-0 (black curve), MM REHE-200 (red curve) and REHE-600 (blue curve) samples

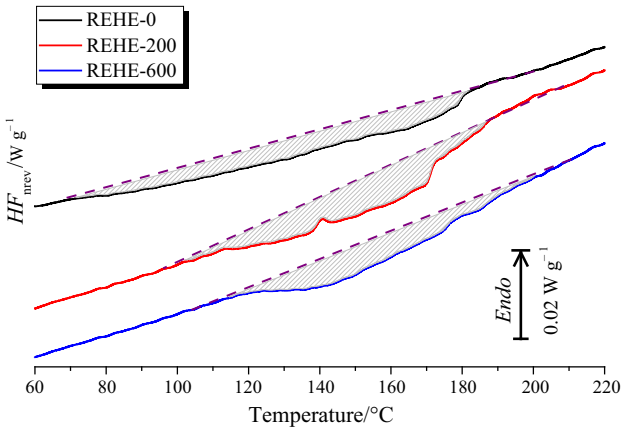

Fig. 7 Modulated DSC profile (TOPEM®) showing low-temperature pre-T_g exotherms in non-reversing heat flow HF_{nrev} for coarse-grained powdered REHE-0 (black curve), MM REHE-200 (red curve) and REHE-600 (blue curve) samples

The observed decaying trend in ΔC_{p0} for amorphous phase with high-T_{g1} glass transition midpoint (with growing rotational speed n) testifies that low-T_{g2} amorphous phase is formed under MM from this high-T_{g1} phase (which exist just before MM in REHE-0 sample) in addition to amorphous phase vitrified from β-As_4S_4 crystallites. Thus, the overall solid-state amorphization in commercial arsenic sulfide subjected to high-energy MM occurs from two sources, these being high-to-low-T_g amorphous phase transformation and direct vitrification of β-As_4S_4 crystallites.

The heterogeneity of chemical environment over inner crystalline phase (β-As_4S_4) results in incongruent double-peak melting distinctly observed near ~ 305 °C and ~ 315 °C (see Fig. 1a). Because of shielding by amorphized

surface, the melting of such crystallites proceeds at higher T_{m2}, as it can be expected from simple thermodynamic consideration. (The amorphous phase is firstly extracted at the grain surface and intergranular regions.) At the same time, the melting of β-As_4S_4 crystallites separated from amorphous phase occurs at lower T_{m1} (near the liquidus in As-S system [23, 24]), strict position of this effect being defined by thermodynamics of a melting system (the effect of melting-point T_{m1} depression in MM arsenicals as compared with non-milled coarse-grained one, see Fig. 5).

This crystal-glass equilibrium can be substantially disturbed due to initial melting (in the first heating–cooling run), when both parent crystalline and amorphous phases become well separated within alloy. Respectively, the specific heat capacity C_{p0} in the second heating run attains character attribute of congruent melting with single-peak T_{m1} approaching 303.4 °C for non-milled REHE-0 and 304.7 °C for MM REHE-500 samples (Fig. 1b). Amorphous phase in these samples becomes compositionally close to arsenic monosulfide (As_4S_4), being presented in the modulated DSC profiles (TOPEM®) in Fig. 2b by single-T_g relaxation event near ∼ 190.3 °C ($\Delta C_{p0} = \sim 0.190$ J g^{-1} K^{-1}) and ∼ 191.3 °C ($\Delta C_{p0} = \sim 0.100$ J g^{-1} K^{-1}) for REHE-0 and MM REHE-500 pellets, respectively. In other words, the effect of high-energy MM-driven depression in the melting temperature T_{m1} is indeed gradually destroyed after samples re-melting.

Continuous generation of amorphous phase under speed-increased high-energy MM in directly synthesized β-As_4S_4 arsenicals testified rather in favor of "shell" kinetic model [4, 5] treated this phenomenon in terms of intensive generation and accumulation of different structural defects in parent crystalline phase. Under these high-energy MM (with speed n not exceeding 600 min^{-1}), the appeared amorphous phase nucleates heterogeneously starting from crystallite grain boundaries, followed by stretching into crystallite grain interior. There were no any abrupt critical size effects in crystallite grains of MM β-As_4S_4 arsenicals allowing collapse of crystalline structure in respect of "the crystallite destabilization model" like in elemental Se [2, 3]. (Crystallites smaller than the critical grain size are transformed completely into amorphous phase, while those larger than the critical size remain crystalline.)

Conclusions

Continuous generation of amorphous phase in addition to parent crystalline β-As_4S_4 one was probed in directly synthesized high-temperature polymorph of tetra-arsenic tetra-sulfide under high-energy mechanical milling with 100–600 min^{-1} rotational speeds. The thermodynamic authenticity of generated amorphous phase was clarified exploring the temperature-modulated DSC TOPEM® method. The crystalline–amorphous heterogeneity of chemical environment proper to β-As_4S_4 results in incongruent double-peak melting revealed in the modulated DSC profiles (TOPEM®) through two endothermic effects at ∼ 305 °C and ∼ 315 °C. The amorphized substance appeared under MM is of dual nature, being represented by As-rich glassy phases possessing high-temperature (∼ 208.3 °C) and low-temperature (∼ 130-140 °C) glass transition midpoints. Such double-T_g relaxation is accepted as indicative of intrinsic separation in the generated amorphized phase. The crystal-glass equilibrium in the milled arsenicals can be substantially modified with repeated melting, when crystalline and glassy phases become well separated, resulting in congruent melting near ∼ 305 °C and single glass relaxation event near ∼ 191 °C. The overall solid-state amorphization in commercial arsenic sulfide subjected to high-energy ball mechanical milling occurs from two sources, these being high-to-low-T_g transformation of existing amorphous phase and direct vitrification of parent β-As_4S_4 phase. These data testifies in favor of "shell" kinetic model treated solid-state amorphization in terms of intensive defect accumulation in β-As_4S_4 phase, the appeared amorphous phase being nucleated heterogeneously from grain boundaries followed by stretching into grain interior.

Acknowledgements This work was supported by the Slovak Research and Development Agency under the contract no. APVV-14-0103 and Slovak Grant Agency VEGA (project 2/0027/14). The publication contains the results of studies conducted by President's of Ukraine grant for competitive projects (F70/134-2017) of the State Fund for Fundamental Research.

References

1. Piot L, Le Floch S, Cornier T, Daniele S, Machon D. Amorphization in nanoparticles. J Phys Chem C. 2011;117:11133–40.
2. Zhao YH, Jin ZH, Lu K. Mechanical-milling-induced amorphization of Se: a crystallite destabilization model. Phil Mag Lett. 1999;79:747–54.
3. Zhao YH, Zhu YT, Liu T. Mechanism of solid-state amorphization of Se induced by mechanical milling. J Appl Phys. 2004;5:7674–80.
4. Benjiamin JS, Schelleng RD. Dispersion strengthened aluminum-4 Pct magnesium alloy made by mechanical alloying. Metall Trans A. 1981;12:1827–32.

5. Schwarz RB, Petrich RR, Saw CK. The synthesis of amorphous NiTti alloy powders by mechanical alloying. J Non-Cryst Solids. 1985;76:281–302.
6. Qiao A, Yang H, Xiao HY, Xiao J, Liu XP, Ge ZR, Chen RH. Milling-induced amorphization in a chalcogenide compound. Chalcogenide Lett. 2017;14:195–201.
7. Deng Y, Xu H, Huang K, Yang X, Xie C, Wu J. Size effects of realgar particles on apoptosis in a human umbilical vein endothelial cell line: ECV-304. Pharm Res. 2001;44:513–8.
8. Dilda PJ, Hogg PJ. Arsenical-based cancer drugs. Cancer Treatment Rev. 2007;33:542–64.
9. Wu J-Z, Ho PC. Evaluation of the in vitro activity and in vivo bioavailability of realgar nanoparticles prepared by cryo-grinding. Eur J Pharm Sci. 2006;29:35–44.
10. Baláž P, Sedlák J. Arsenic in cancer treatment: challenges for application of realgar nanoparticles (a minireview). Toxins. 2010;2:1568–81.
11. Tian Y, Wang X, Xi R, Pan W, Jiang S, Li Z, Zhao Y, Gao G, Liu D. Enhanced antitumor activity of realgar mediated by milling it to nanosize. Int J Nanomed. 2014;9:745–57.
12. Šiljegović MV, Štrbac GR, Skuban F, Lukić-Petrović SR. Determination of thermal parameters of glasses from the system Bi_x $(As_2S_3)_{100-x}$ based on DSC curves. J Therm Anal Calorim. 2011;105:947–51.
13. Golovchak R, Shpotyuk O, Kozdras A, Riley BJ, Sundaram SK, McCloy JS. Radiation effects in physical aging of binary As–S and As–Se glasses. J Therm Anal Calorim. 2011;103:213–8.
14. Šiljegović MV, Lukić-Petrović SR, Štrbac GR, Petrović DM. Kinetic analysis of the crystallization processes in the glasses of the Bi–As–S system. J Therm Anal Calorim. 2012;110:379–84.
15. Holubová J, Černošek Z, Černošková E. Thermal properties and structure of $(As_2S_3)_{100-x}(Sb_4S_4)_x$ glassy system. J Therm Anal Calorim. 2014;116:699–702.
16. Shpotyuk O, Kozdras A, Demchenko P, Shpotyuk Y, Bujňáková Z, Baláž P. Solid-state amorphization of $As_{45}S_{55}$ alloy induced by high-energy mechanical milling. Thermochim Acta. 2016;642:59–66.
17. Bujňáková Z, Baláž P, Makreski P, Jovanovski G, Čaplovicová M, Čaplovič L, Shpotyuk O, Ingram A, Lee T-C, Cheng J-J, Sedlák J, Turianicová E, Zorkovská A. Arsenic sulfide nanoparticles prepared by milling: properties, free-volume characterization, and anti-cancer effects. J Mater Sci. 2015;50:1973–85.
18. Baláž P, Baláž M, Shpotyuk O, Demchenko P, Vlček M, Shopska M, Briančin J, Bujňáková Z, Shpotyuk Y, Selepová B, Balážová L. Properties of arsenic sulphide (β-As_4S_4) modified by mechanical activation. J Mater Sci. 2017;52:1747–58.
19. Shpotyuk O, Bujňáková Z, Baláž P, Ingram A, Demchenko P, Kovalskiy A, Vlcek M, Shpotyuk Y, Cebulski J, Dziedzic A. Nanostructurization effects in PVP-stabilized tetra-arsenic tetrasulfide As_4S_4 nanocomposites. Mater Chem Phys. 2017;186:251–60.
20. Schawe JEK, Hutter T, Heitz C, Alig I, Lellinger D. Stochastic temperature modulation: a new technique in temperature-modulated DSC. Thermochim Acta. 2006;446:147–55.
21. Fraga I, Montserrat S, Hutchinson J. TOPEM, a new temperature modulated DSC technique. Application to the glass transition of polymers. J Therm Anal Calorim. 2007;87:119–24.
22. Jonker WPA. Untersuchungen uber das System: Schwefel und Arsen. Z Anorg Chem. 1909;62:89–107.
23. Hrubý A. A study of glass-forming ability and phase diagram of the As–S system. J Non-Cryst Solids. 1978;28:139–42.
24. Blachnik R, Hoppe A, Wickel U. Die systeme Arsen-Schwefel und Arsen-Selen und die thermodynamischen Daten ihrer Verbindungen. Z Anorg Allg Chem. 1980;463:78–90.
25. Street GB, Munir ZA. The structure and thermal properties of synthetic realgar (As_4S_4). J Inorg Nucl Chem. 1970;32:3769–74.
26. Chattopadhyay TN, Gmelin E, von Schnering HG. Heat capacity study of the phase transitions in As_4S_3 and As_4S_4. Phys Stat Solidi A. 1983;76:543–51.
27. James PF. Review. Liquid-phase separation in glass-forming systems. J Mater Sci. 1975;10:1802–25.
28. Myers M, Berkes JS. Phase separation in amorphous chalcogenides. J Non-Cryst Solids. 1972;8–10:804–15.
29. Takagi M. Electron-diffraction study of liquid-solid transition of thin metal films. J Phys Soc Jpn. 1954;9:359–63.
30. Nanda KK, Sahu SN, Behera SN. Liquid-drop model for the size-dependent melting of low-dimensional systems. Phys Rev A. 2002;66:013208.
31. Farrell HH, Van Siclen CD. Binding energy, vapor pressure, and melting point of semiconductor nanoparticles. J Vac Sci Technol, B. 2007;25:1441–7.
32. Shpotyuk O, Bujňáková Z, Sayagués MJ, Baláž P, Ingram A. Shpotyuk Ya, Demchenko P. Microstructure characterization of multifunctional As_4S_4/Fe_3O_4 nanocomposites prepared by high-energy mechanical milling. Mater Charact. 2017;132:303–11.
33. Bujňáková Z, Shpotyuk O, Sedlák J, Pastorek M, Turianicová E, Baláž P, Ingram A. Physico-chemical and biological properties of arsenic sulfide ($As_{55}S_{45}$) nanosuspension prepared by milling. Acta Phys Pol, A. 2014;126:902–6.
34. Pagacz J, Pielichowski K. PVC/MMT nanocomposites. DSC with stochastic temperature modulation study at glass transition region. J Therm Anal Calorim. 2013;111:1571–5.
35. Shah N, Iyer RM, Mair H-J, Choi DS, Tian H, Diodone R, Fahnrich K, Pabst-Ravot A, Tang K, Scheubel E, Grippo JF, Moreira SA, Go Z, Mouskountakis J, Louie T, Ibrahim PN, Sandhu H, Rubia L, Chokshi H, Singhal D, Malick W. Improved human bioavailability of vemurafenib, a practically insoluble drug, using an amorphous polymer-stabilized solid dispersion prepared by a solvent-controlled coprecipitation process. J Pharm Sci. 2013;102:967–81.
36. Myers MB, Felty EJ. Structural characterizations of vitreous inorganic polymers by thermal studies. Mater Res Bull. 1967;2:535–46.
37. Feltz A. Amorphous Inorganic Materials and Glasses. New York: VCH Publ; 1993.